Japanese Journal of Applied Physics
Vol. 46, No. 8B, 2007, pp. 5607–5610

Electrical Properties of Single Carbon Nanofibers Grown on Tips of Scanning Probe Microscope Cantilevers by Ion Irradiation

Masashi KITAZAWA[1,2*], Ryo OHTA[1], Junya TANAKA[2], and Masaki TANEMURA[2]

[1]*Olympus Co., Ltd., Tatsuno, Nagano 399-0495, Japan*
[2]*Department of Environmental Technology, Graduate School of Engineering, Nagoya Institute of Technology, Nagoya 466-8555, Japan*

(Received January 19, 2007; accepted April 11, 2007; published online August 23, 2007)

The Ar ion irradiation method has a high potential for the batch fabrication of single carbon nanofibers (CNFs) onto the tip of cantilevers, and is known to have excellent mechanical characteristics. In this study, we analyzed the electrical properties of ion-induced CNFs. For this purpose, current–voltage (I–V) properties were measured using an atomic force microscope (AFM). Commercial-type Si probes (without CNFs) showed a typical diode characteristic. By contrast, Si probes with ion-induced CNFs (CNF probes) showed a metallic characteristic similar to that of Pt-coated Si probes. The Pt-coated Si probes were completely damaged at an applied voltage of 5 V, whereas the CNF probes retained their metallic I–V characteristic and no increase in resistance was detected even at 10 V. Electrical properties were further investigated by scanning spreading resistance microscopy (SSRM) measurements. Compared with electroconductive diamond probes, which are commonly used for SSRM measurements, CNF probes were superior in the sensitivity for measuring surface roughness owing to both the small radial curvature of the tip and a high aspect ratio. Thus, it was believed that the CNF probes are quite promising as electroconductive probes. [DOI: 10.1143/JJAP.46.5607]

KEYWORDS: scanning probe microscope (SPM), atomic force microscope (AFM), carbon nanofiber (CNF), carbon nanotube (CNT), scanning spreading resistance microscopy (SSRM), electroconductive probes

1. Introduction

Since the development of a scanning tunnel microscope (STM) by Binnig *et al.*, a scanning probe microscope (SPM) is one of the most powerful surface analysis devices used in various fields ranging from basic research to industrial applications.[1)] Thus, the physical surface phenomena of friction,[2)] magnetism,[3,4)] and electric characteristics[5–8)] have been captured by SPM technologies. From the viewpoint of practical applications, SPM probes should possess sufficient durability and mechanical strength. In addition, the importance of electroconductive probes has increased in nanotechnology fields.

For the measurements of the electrical properties of sample surfaces, in general, metal-coated Si or electroconductive diamond probes are used. Unfortunately, the former cannot tolerate for large current, whereas the latter is not very sensitive in for measuring surface roughness owing to the round tip shape. In addition, diamond probes frequently damage the sample surface because of the hardness of the tip. Thus, the development of probes with high electric conductivity, sharp-tip radius, and high flexibility is indispensable.

In our previous paper, we reported that single carbon nanofibers (CNFs) can be grown onto commercial-type Si SPM cantilevers using an ion irradiation method.[9)] Additionally, the ion-induced CNF probes that were small-scale batch-fabricated were demonstrated to possess mechanical properties similar to those of high-quality carbon nanotube (CNT) probes.[10,11)] In this report, in order to explore the potential of ion-induced CNF probes as an electroconductive cantilever, their electrical properties were investigated in detail using atomic force microscopy (AFM) and scanning spreading resistance microscopy (SSRM)[12)] methods.

*E-mail address: ma_kitazawa@ot.olympus.co.jp

2. Experimental Procedure

2.1 Nanofabrication system

For the fabrication of CNF probes, we employed commercially available SPM cantilevers (see below also). After coating a thin carbon layer, the probes were ion-irradiated using a Kaufman-type ion gun, 3 cm in ion-source diameter, in a nanofabrication system. The growth mechanism of ion-induced CNFs is described in detail elsewhere.[13)] In brief, CNF growth is due to the redeposition of sputter-ejected carbon atoms onto the sidewall of conical protrusions and the excess surface diffusion of the carbon atoms to the tips during Ar^+ sputtering. The Ar^+-ion-beam energy employed for ion-induced CNF growth was 600 eV, and the growth duration was about 10 min. The basal and working pressures were 1.5×10^{-5} and 2×10^{-2} Pa, respectively. Several CNFs probes can be fabricated simultaneously in a batch process.

2.2 Cantilevers

The cantilevers used were the tetrahedral type (Olympus OMCL-AC240TS, $L \times W \times T = 240 \times 30 \times 2.7\,\mu m^3$) of Si. They are characterized by having the "tip-view structure" where the tip is formed at a free edge of a cantilever. CNFs, 500 nm in length and 30 nm in diameter were formed on the tips by above-described Ar^+ ion irradiation method. CNF length was controlled by growth time, and the discrepancy in length was typically ±10% in an array of nine SPM chips batch-grown under the above-described conditions.[14)] For I–V measurements the above-described Si cantilevers, which are N-type and possess a bulk resistance of 4–6 Ω cm, Pt-coated Si cantilevers (OMCL-AC240TM, $L \times W \times T = 240 \times 30 \times 2.7\,\mu m^3$), whose resitivity is 52×10^{-6} Ω cm, and the diamond probes (CDT-NCHR, $L \times W \times T = 125 \times 30 \times 4.0\,\mu m^3$) were also employed for comparison. The tip radius of the Pt-coated probes was 25 nm or smaller. The diamond probes are generally used as electroconductive probes in SSRM measurements, and are com-

Table I. Characteristics and size of cantilevers employed in this study.

	Method			
	AC240TS	Ion-induced CNF	AC240TM	CDT-NCHR
Lever dimension $L \times W \times T$ (μm^3)	$240 \times 30 \times 2.7$	$120 \times 30 \times 3.7$	$240 \times 30 \times 2.7$	$125 \times 30 \times 4.0$
Resonant frequency (kHz)	70	285	70	320
Probe material	Silicon	Amorphous C	Pt/Si (20 nm)/Si	Doped diamond (100 nm)/Si
Resistivity (Ω cm)	4–6	(1.375×10^{-3})	10.6×10^{-6}	4×10^{-3}
Tip/probe height (μm)	14	14/0.7	14	14
Radius of curvature (nm)	7	15	25	150

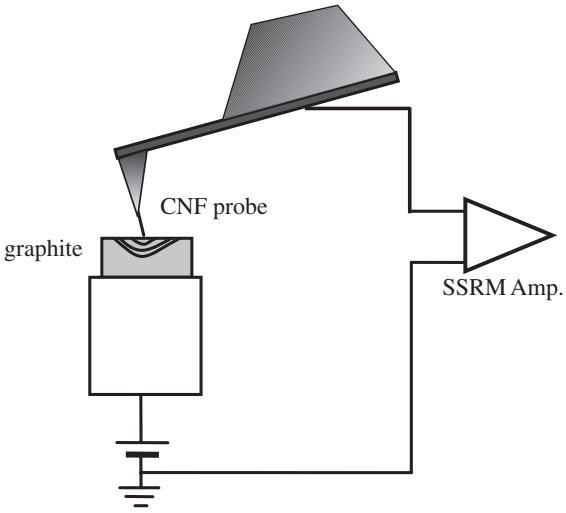

Fig. 1. Schematic diagram for SSRM measurements.

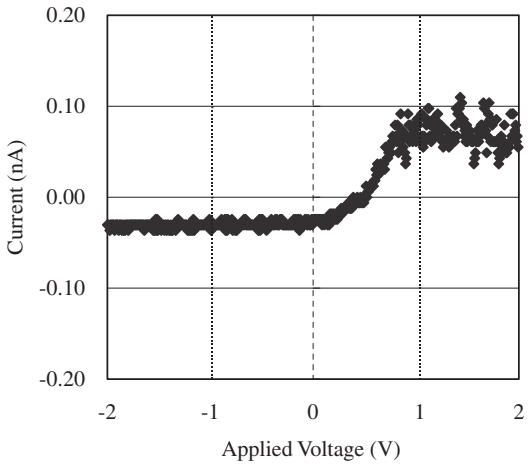

Fig. 2. *I–V* characteristic attained for a commercial-type Si probe.

posed of a Si coated with B-doped diamond film, 100 nm in thickness. The resistivity and the radius of the diamond probes were 100–200 nm and 0.003–0.005 Ω cm, respectively. The characteristics and the size of the cantilevers are shown in Table I.

2.3 *Evaluation*

I–V measurements were performed using AFM (SII-NT E-Sweep). The probes were contacted with a graphite sample surface gently (approximately 100 nN). Because the graphite surface was rugged, the *I–V* measurements were carried out at different two points and reproducibility was confirmed. The voltage applied was scanned from negative to positive on the probe side.

The electrical property of CNF probes was further investigated by SSRM methods, in which the resistance of the graphite surface was measured using AFM in the contactmode. The circuit diagram employed is shown in Fig. 1. For the SSRM measurements, the probes were contacted with the graphite surface strongly (approximately 2000 nN). The bias voltage applied was -0.5 V, and the scan area was set at $500 \times 125\,nm^2$. The other measurement conditions were as follows: I gain/P gain $= 0.235/0.007$, scan speed $= 0.6$ Hz, and screen ruling $= 512/32$. After the SSRM measurements, the change in the probe shape was observed in detail using a field emission scanning electron microscope (FE-SEM; Hitachi S-4700).

3. Results and Discussion

The *I–V* characteristic obtained for a commercial-type Si probe is shown in Fig. 2, showing a typical diode characteristic. As shown in Fig. 2, the maximum current attainable was in the order of picoampere, owing to the high resistivity of the Si probe. From Fig. 2, the total resistance composing those of the material itself, the contact and the circuit system, was estimated to be 20 GΩ at an applied voltage of 1 V.

Figure 3(a) shows the *I–V* curves measured in the range of ± 1 V for a Pt-coated Si probe (Pt thickness: 20 nm), showing a metallic property. The resistance was estimated to be 10 MΩ from the inclination of the straight line. In order to determine the high-current performance of this probe, the applied voltage was further increased to 5 V. As shown in Fig. 3(b), however, almost no current was detected, perhaps owing to the damage of the probe. After this damage, current was no longer detected even in an applied voltage range of ± 1 V. In order to examine the physical damage, the probe was observed using FE-SEM after the *I–V* measurement. As was expected, the tip region was completely damaged. As shown in Fig. 4, the coated Pt film seemed to be molten owing to the excess current applied.

Figure 5(a) shows the *I–V* characteristic obtained for a CNF probe in an applied voltage range of ± 1 V, revealing a metallic property similar to that attained for the Pt-coated Si probe. The resistance was estimated to be 2 MΩ from the inclination of the straight line. A further increase in applied voltage to 10 V yielded no change in the *I–V* characteristic (inclination). The actual current was larger than 1 μA at 10 V. The reliability of the CNF probes was confirmed when a voltage of ± 50 mV was applied again; no change was detected in the *I–V* characteristic before and after this high-

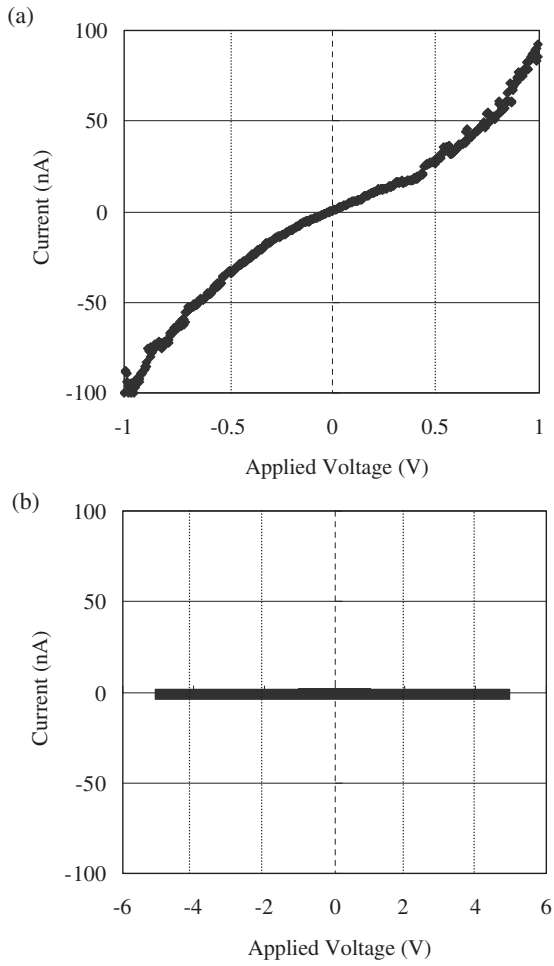

Fig. 3. *I–V* characteristic attained for a commercial-type Pt-coated Si probe. Applied voltage range: (a) ±1 and (b) ±5 V.

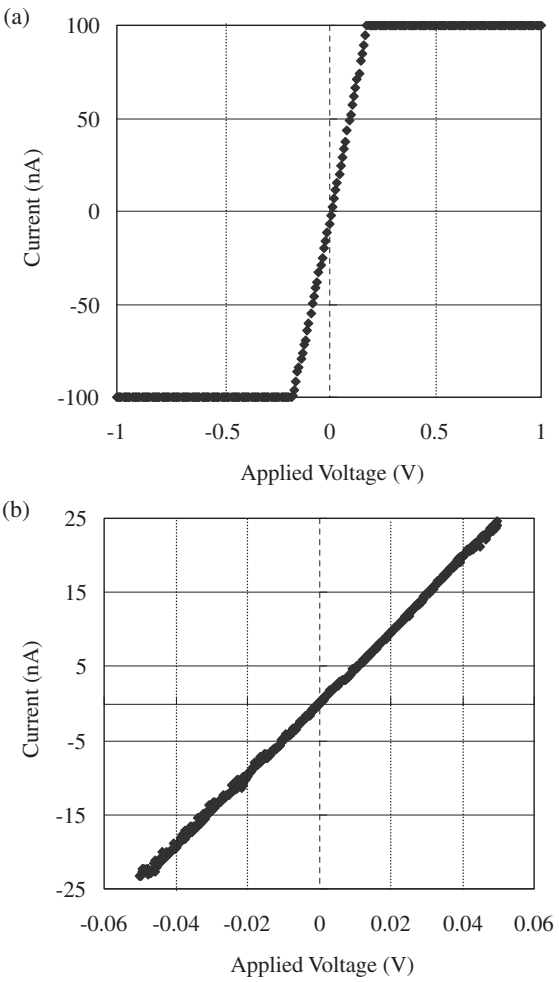

Fig. 5. *I–V* characteristic obtained for a CNF probe. Applied voltage range: (a) ±2 and (b) ±50 mV.

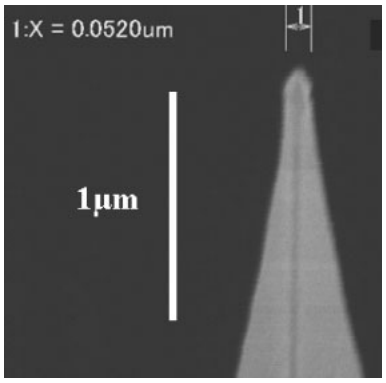

Fig. 4. SEM image of the Pt-coated probe taken after the *I–V* measurement.

current application [Fig. 5(b)]. In order to determine the difference in electrical property between CNF probes, three additional CNF probes were also tested. These CNF probes showed almost identical metallic *I–V* characteristics. Thus, the metallic property was common to CNF probes. In addition, no change in probe morphology was also observed using FE-SEM before and after the high-current application.

The electrical properties of CNF probes were further investigated using the SSRM method. For comparison, the measurement was carried out also using electroconductive diamond probes, which are commonly used for SSRM analysis, and Si probes. Figures 6(a)–6(c) show the topography of a graphite surface ($500 \times 150\,\mathrm{nm}^2$) measured using diamond, Si and CNF probes, respectively. For the measurement using diamond probe, the measured average resistance on the surface and the surface roughness (rms value) were about 250 kΩ and 13.3 nm, respectively [Fig. 6(a)]. For the measurement using the Si probe, because of the high resistivity of the Si probe itself, the measured resistance was as high as 4 GΩ, and the measured rms value was 15.8 nm, which was smaller than that expected from the original probe-tip sharpness [Fig. 6(b)]. Because the contact between the probe and the graphite surface was high in the SSRM analyses, the tip shape was thought to be round during the measurement.

For the measurement using the CNF probe, the average resistance and rms values measured were of about 3 MΩ and 50.4 nm, respectively [Fig. 6(c)]. The rms value was the largest for the CNF probe. This may be due to the tip sharpness, high aspect ratio and durability against the hard contact of the CNF probe against the sample surface.

After the SSRM measurements, the shape of the probes was observed using SEM. As shown in Fig. 7, no difference in length or shape was observed before and after the SSRM

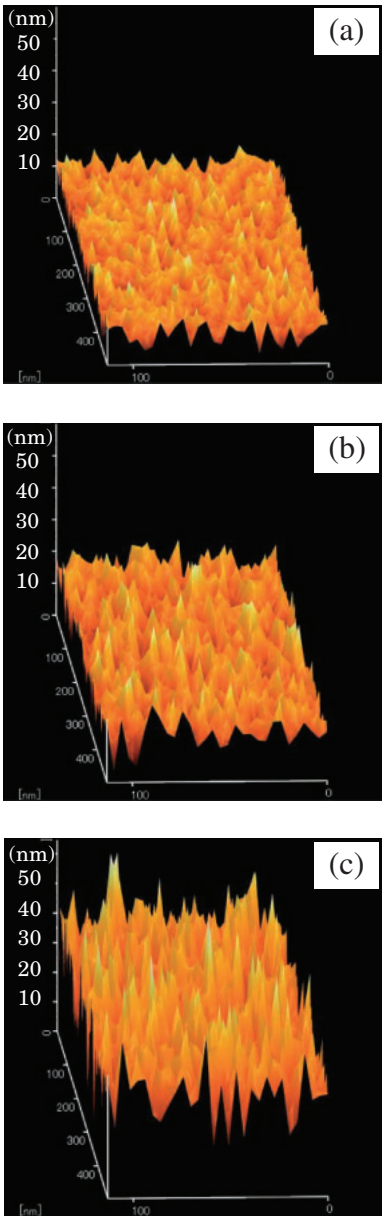

Fig. 6. Surface roughness profiles of a graphite in the SSRM measurements obtained using (a) diamond probe, (b) Pt-coated Si probe, and (c) CNF probe.

measurements using the diamond and CNF probes, whereas the Si tip was observed to be flattened after the SSRM measurements, as was predicted above.

In the SSRM measurements, the probe contacts with the sample surface strongly. Under such a condition, the sharper the tip, the greater the local stress applied to the contacted sample surface with the probe. This may lead to damage on the sample surface. Owing to the flexibility of CNFs, however, less damage will be formed in the case of using CNF probes.

The resistance obtained for the CNF probe was higher than that attained for the conventional diamond probe. This may be due to the amorphous nature of CNFs. Thus, for the better performance of CNF probes as electroconductive probes, the control of the crystalline structure of CNFs will be important. Experiments along this line are now being undertaken, and the results will be reported in a forthcoming paper.

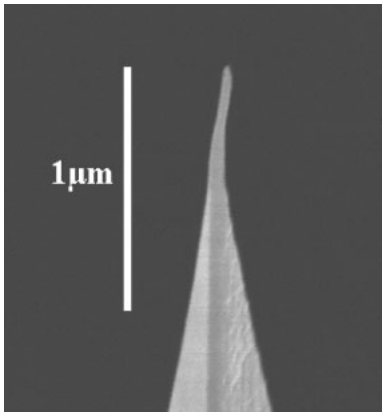

Fig. 7. SEM image of the CNF probe taken after SSRM measurement.

4. Conclusions

Ion-induced CNF probes were metallic in electrical property, and were applicable to high-current measurements. Because the CNF probes possessed a sufficient tip sharpness, a high aspect ratio, and durability against a strong contact with the sample surface, their excellent performance was demonstrated for SSRM measurements, which are difficult to attain using conventional Si or metal-coated Si probes. Thus, it was concluded that ion-induced CNFs are promising as practical conductive SPM probes.

Acknowledgements

This work was partially supported by the Japan Science and Technology Agency (JST; Grant-in-Aid for Development of Systems and Technology for Advanced Measurement and Analysis), the Japan Society for the Promotion of Science (JSPS; Grant-in-Aid for Scientific Research B, No. 18360022), and a grant from the NITECH 21st Century COE Program "World Ceramics Center for Environmental Harmony."

1) G. Binnig, H. Rohrer, Ch. Gerber, and E. Weibel: Phys. Rev. Lett. **49** (1982) 57.
2) J. Ruan and B. Bhushan: J. Tribol. **116** (1994) 378.
3) Y. Martin and H. K. Wickramainghe: Appl. Phys. Lett. **50** (1987) 1455.
4) P. Rice and J. Moreland: IEEE Trans. Magn. **27** (1991) 3452.
5) J. J. Kopanski, J. F. Marchiando, and J. R. Lowney: J. Vac. Sci. Technol. B **14** (1996) 242.
6) M. Nonnenmacher, M. P. O'Boyle, and H. K. Wickramasighe: Appl. Phys. Lett. **58** (1991) 2921.
7) J. E. Stern, B. D. Terris, H. J. Mamin, and D. Ruger: Appl. Phys. Lett. **53** (1988) 2717.
8) M. Kitazawa and A. Toda: Jpn. J. Appl. Phys. **41** (2002) 4928.
9) M. Tanemura, M. Kitazawa, J. Tanaka, T. Okita, R. Ohta, L. Miao, and S. Tanemura: Jpn. J. Appl. Phys. **45** (2006) 2004.
10) *Springer Handbook of Nanotechnology*, ed. B. Bhushan (Springer-Verlag, Berlin, 2003) Chap. 21.
11) S. Akita, H. Nishijima, Y. Nakayama, F. Tokumasu, and K. Takeyasu: J. Phys. D **32** (1999) 1044.
12) P. De. Wolf, T. Clarysse, W. Vandervorst, L. Hellemans, Ph. Niedermann, and W. Hanni: J. Vac. Sci. Technol. B **16** (1998) 355.
13) M. Tanemura, J. Tanaka, K. Itoh, Y. Fujimoto, Y. Agawa, L. Miao, and S. Tanemura: Appl. Phys. Lett. **86** (2005) 113107.
14) M. Tanemura, J. Tanaka, M. Kitazawa, and R. Ohta: to be published in J. Phys.: Conf. Ser. (2007).